µFLU14-73

LOCAL THERMO-HYDRODYNAMICS OF A LIQUID PLUG PULSATING INSIDE A DRY CAPILLARY TUBE

Sushant Kumar[1], Balkrishna Mehta[2], Ashish Bajpai[2], Sameer Khandekar[*2]
[1]Birla Institute of Technology and Science Pilani - Goa Campus, Zuarinagar 403726 (Goa) India
sushant08kr@gmail.com
[2]Indian Institute of Technology Kanpur, Kanpur 208016 (UP) India
baluk@iitk.ac.in, ashishkb007@gmail.com, samkhan@iitk.ac.in

KEY WORDS

Liquid slug flow, Pulsating heat pipe, Capillary tube, Time-averaged Nusselt Number

ABSTRACT

Taylor-bubble flow is one of the most important two-phase flow patterns, which belongs to a class of intermittent flows. Because of their unique flow features, such intermittent flows have proved to be promising for augmenting local heat transfer compared to single component flows. One application of such flows is the pulsating heat pipe (PHP), wherein thermally induced self-sustained oscillations of two-phase capillary slug flow takes place; the slugs having a net translational motion coupled with local flow oscillations. In this work, the numerical simulations of the flow of a single isolated liquid slug (of water), pulsating inside a capillary tube of inner diameter = 2.0 mm, is reported. Simulations have been carried out for four different Womersley Numbers ($Wo = R\sqrt{\omega/\upsilon}$) i.e., Wo = 2.35, 3.32, 4.7 and 6.65 which covers the frequency range of 0.44-7 Hz (which, incidentally, is typical for the operation of PHPs). The Capillary number ($Ca = \mu U/\sigma$) is 0.001 for all the cases, with the length-to-diameter (L/D) ratio as 2. The effect of pulsations on the thermo-hydrodynamics is discussed and the importance of correctly defining the Nusselt number is highlighted. It is found that there is a marginal enhancement in the thermal transport due to the imposed pulsations, as compared to steady flow; rather, there can be an overall reduction in Nusselt number too, which can happen at low imposed frequencies. An interesting result is observed wherein the estimated value of the local instantaneous Nu as per the classical definition may come out to be 'negative', due to the crossover of the wall temperature and mean fluid temperature. This happens due to the unique flow characteristics coupled with the thermal boundary layer development in the plug translating with imposed flow pulsations.

1. INTRODUCTION

The last five decades have seen a drastic evolution in the techniques used for efficient thermal management of electronics. Apart from the existing two-phase cooling technologies which comprise pool boiling, spray/mist cooling, flow boiling, liquid jet impingement etc., special technologies like thermoelectric devices and various kinds of heat pipes have gained more prominence over the years. The capability of heat pipes to remove large quantities of heat with a minimal temperature drop has made them highly popular in electronics thermal management. Of these, the Pulsating Heat Pipe (PHP), due to some inherent advantages over the conventional heat pipes has carved a niche for itself. The usage of wicks in conventional heat pipes engenders its own performance limitation in the form of the capillary limit. Other limitations include the viscous, the sonic, the entrainment and the boiling limit. The simple design which obviates the need for a wick makes PHPs more reliable, cost effective and easy to manufacture. In the last decade, active research has been done in understanding the complex internal two-phase thermo-hydrodynamics of PHPs [1-4]. In a PHP, self-sustained thermally driven oscillations of bubbles and slugs (Taylor slug-bubble flow) take place.

[*] Corresponding author: samkhan@iitk.ac.in

Hence, to make a complete analysis of the PHPs, we need to understand the thermo-hydrodynamic characteristics of these pulsating/oscillating slug flows in small diameter capillary tubes.

Khandekar [2] and Zhang and Faghri [5] showed that about 90% of the heat transfer in PHPs takes place between the tube wall and liquid slugs in the form of single-phase heat transfer (i.e. sensible heating) and the remaining 10% is due to the evaporation and condensation of the working fluid (i.e. by latent heat). Accordingly an acceptable analysis can be made considering the flow to be in the non-phase-change domain, wherein no condensation or evaporation from the meniscus is taking place. Hence, considering sensible heat as the primary mechanism of heat transfer in PHPs, an otherwise complex system can be simplified to a non-boiling pulsating Taylor slug flow.

Experimental investigation of heat transfer in non-boiling two-phase slug flow in a circular channel of diameter 1.5 mm using Infrared Thermography (IRT) was reported by Walsh et al. [6]. The study revealed that such flows could be highly efficient in enhancing heat transfer, as compared to the fully developed single-phase flows. Several numerical studies of Taylor slug flow were also reported in recent times, which highlighted the effect of *L/D, Pr, Ca*, on the heat transfer and shear stress (for example, see Gupta et al. [7]; Asadolahi et al. [8]; Bajpai and Khandekar [9]).Mehdizadeh et al. [10]) performed detailed computational simulations using the VOF method, including the thin film surrounding the gas bubble, and reported an overall enhancement of up to 610% in heat transfer. Existence of three-dimensional nature of flow, especially for $Re_{TP} \geq 950$ has also been highlighted, for example, by Asadolahi et al. [11] and Talimi et al. [12]. Recent micro-PIV studies on circular and non-circular channels clearly revealed the flow re-circulations inside the liquid slugs and the effect of gravity on film thickness and heat transfer (Leung et al. [14]; Zaloha et al. [15]).

Talimi et al.[12,13] simulated slug flow heat transfer in both, circular and square microchannels using single-phase Moving Frame Reference (MFR), where the unit cell comprised of a liquid slug/plug. Though thin liquid films are generally found in microchannels, the film and its effects were neglected, i.e., a dry slug was considered. It was concluded that MFR technique over predicts the pressure drop. The heat transfer in dry slugs is higher than in wet slugs because of the negative effect of liquid films on thermal boundary layer and amount of liquid circulations. Thus, it was concluded that microchannel heat sinks working in dry slug flow condition would provide greater heat transfer enhancement.

Zhang et al. [5] numerically investigated the liquid-vapor pulsating flow in a vertically oriented miniature U-tube. It was concluded that the initial displacement of the liquid slug and gravity has no effect on the amplitude and angular frequency of the oscillations. In another fundamental study, Das et al. [16] and Rao et al. [3] experimentally observed the thermo-hydrodynamics of thermally induced meniscus oscillations in a two-phase system consisting of a liquid slug and a vapor bubble in a capillary tube. Such a system can develop an instability that leads to self-sustained auto oscillation of meniscus. Displacement of meniscus and pressure variations was analyzed close to instability and far from it. It was found that close to instability, oscillations were less regular with relatively smaller amplitude than the oscillations far from instability.

Most recently, Mehta and Khandekar [17] made an attempt to study the heat transfer characteristics of pulsating Taylor bubble-train flow in square minichannels using IRT. They concluded that perturbing the Taylor bubble-train flow causes greater disturbances in the wakes of the bubbles, which may conditionally lead to enhancement in the heat transfer over continuous Taylor bubble-train flow. However, due to the limitation of not being able to determine the local bulk fluid temperature, they could not make a detailed analysis of the mechanism of heat transfer and local heat transfer coefficient in pulsating Taylor bubbles.

In this background, numerical simulations of the flow of a single isolated liquid slug pulsating uni-directionally inside a round capillary tube of internal diameter 2.0 mm, is reported here. The working fluid considered is water. Generally, one would find thin liquid films around the oscillating bubbles in a PHP but here, like in Talimi et al. [12,13], dry slug flow is considered. Simulations have been carried out for four different non-dimensional frequency parameter Wo = 2.35, 3.32, 4.70 and 6.65 which cover the frequency range of 0.44-7 Hz. This frequency range is typically found in a PHP. The non-dimensional amplitude of pulsations is 1 and the L/D ratio is kept as 2.

2. PROBLEM FORMULATION AND SIMULATION METHODOLOGY

2.1 Problem Description

Figure 1 (a) shows the problem under consideration. An isolated liquid slug of length L is moving inside a dry capillary tube of radius R. Values are chosen such that the Bond number $Bo < 2$. In such a scenario, the effect of gravity can be neglected as only surface tension dominates. To include the effect of surface tension, advancing and receding menisci are formed using the static contact angles, which are determined experimentally, as will be shown later. It is necessary to clear the difference between oscillating and pulsating flow. In oscillating flow, liquid slug does not have any mean flow; hence slug only oscillates with the imposed frequency (refer Figure 1 (b)). On the other hand, in pulsating flow, slug is moving with a net mean flow while an oscillating velocity is superimposed on the flow. The present work analyses only pulsating flows i.e. the slug is moving with a net translational velocity along with oscillations. Hence, the velocity of the slug can be written as $U(1+sin\ \omega t)$ which has two components, a translational velocity U and an oscillating component $U\ sin\ \omega t$. Hence, the velocity of the plug can also be written as:

$$u = U + u' \tag{1}$$

where U is the net mean velocity in axial direction while u' is the fluctuating component of velocity. Similarly pressure-gradient can be written as:

$$\left(\frac{dp}{dx}\right)_{pulsating} = \frac{dp}{dx} + \left(\frac{dp}{dx}\right)' \tag{2}$$

where $(dp/dx)'$ shows the oscillating component. Hence, from here onwards, unless otherwise stated, a (') superscript denotes the fluctuating component of corresponding variable.

The walls of the tube are supplied with a constant heat flux q''. Problem is solved as 2D axis symmetric transient problem to understand the basic thermo-hydrodynamics. For simulation, the wall is given a negative velocity equal to the real fluid's velocity while fluid zone is kept stationary, hence giving a positive relative velocity to the fluid with respect to the wall. All plots and figures from here onwards are presented from the perspective of an observer in the moving frame of reference.

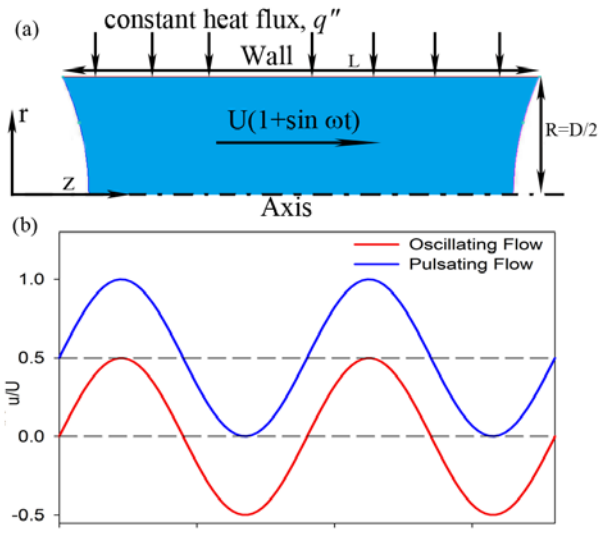

Figure 1: (a) Pulsating slug problem under consideration. The slug is moving with a net translational velocity along with imposed oscillations; the problem is solved with 2D axis-symmetric approximation. (b) Waveform for oscillating flow and pulsating flow.

2.2 Determination of advancing and receding contact angles

It is known that due to the interplay between the capillary and viscous forces during the motion of the meniscus, dynamic contact angles are formed between the liquid meniscus and solid surface which are different from the static equilibrium contact angles. This phenomenon is called contact angle hysteresis. The effect of contact angle hysteresis on heat transfer was analyzed by Bajpai & Khandekar [9]. According to the

Hoffman-Tanner's law, the dynamic contact angles are a function of *Ca* and the initial static contact angle. But as stated before, in this problem the slug is moving with a time dependent velocity. Hence, for each time step of the simulation, the *Ca* would change, leading to a different contact angle for each step. In the present numerical methodology, the contact angle cannot be changed at each time step. So, the static and dynamic contact angles are assumed to be same as the initial static contact angles. As posited by Bajpai and Khandekar [9], because of contact angle hysteresis the rear curve becomes more curved than the front one, which in turn makes the circulations and vortex strength at the rear end stronger. This leads to higher heat transfer. On the other hand, for the case of constant contact angles the vortices are symmetric and of poorer strength and consequently, exhibits lower heat transfer. Even though we would not be able to study the asymmetric nature of the vortices formed and the variation of the shape of the two menisci with time, we can get a very vivid understanding of the mechanism of heat transfer and the effect of pulsations using the present methodology.

To determine the initial static contact angle of the working fluid, water was carefully introduced in dry capillary tubes so as to produce isolated single slug. The capillary tubes were made of pyrex glass of inner diameter 2.0 mm and were thoroughly cleaned, rinsed and dried before the experiment. Images were captured using high resolution camera (Photron®-Fastcam-SA3). Figure 2 (a) shows the captured image with the static contact angles at the two interfaces. Based on this measurement, the average static contact angle for water was taken as 67° in the present study.

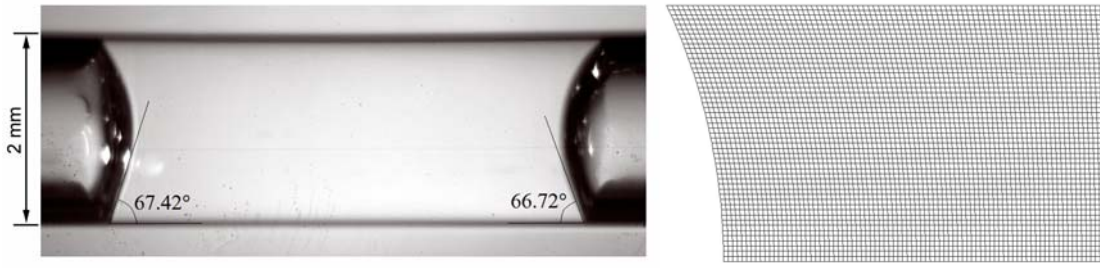

(a) (b)

Figure 2: (a) Captured image of a water liquid slug inside a dry capillary tube of inside diameter 2.0 mm. (b) A Section the computational domain used in this study.

2.3 Governing equations

For all practical purpose, flow is assumed to be incompressible and the mean Reynolds number is chosen in such a way so as to keep the flow in the laminar regime. Hence, 2D governing equations with constant properties can then be written as:

Continuity equation:

$$\nabla.\mathbf{v} = 0 \tag{3}$$

Momentum equation:

$$\rho\left(\frac{\partial \mathbf{v}}{\partial t} + \mathbf{v}.\nabla\mathbf{v}\right) = -\nabla p + \mu\nabla^2\mathbf{v} \tag{4}$$

Energy equation:

$$\rho c_p\left(\frac{\partial T}{\partial t} + \mathbf{v}.\nabla T\right) = k_f\nabla^2 T \tag{5}$$

Distance and velocities are non-dimensionalized as follows (refer Figure 1 (a)):

$$r^* = \frac{r}{R}\ ;\ z^* = \frac{z}{R}\ ;u^* = \frac{u}{U}\ ;v^* = \frac{v}{U}$$

where u is the axial velocity, v is the radial velocity, r and z are the spatial coordinates, r^* and z^* are non-dimensional spatial coordinates; R is the radius of the tube and U is average velocity. Since a constant heat flux boundary condition has been imposed, the temperature is non-dimensionalized as:

$$T^* = \frac{T}{q^{"}r/k_f}$$

Boundary Conditions:
at the wall:

$$u = -U(1+\sin\omega t) \tag{6}$$

and

$$q" = \text{constant} \tag{7}$$

at the interfaces:

$$q" = 0 \tag{8}$$

and

$$\tau = 0 \text{ (Interface boundary condition)} \tag{9}$$

2.4 Numerical Methodology

The simulations are carried out using a pressure based solver in Ansys® Fluent15.0 for *Wo* = 2.35, 3.32, 4.7 and 6.65 (frequency ~ 0.44 -7.0 Hz) using the Lagrangian approach. PISO algorithm is used for pressure-velocity coupling because of its faster convergence and better accuracy. Green-Gauss Cell Based method is used for calculating gradients while Standard method is used for computing the face pressure. The momentum and energy equations are solved using the second order upwind scheme while the transient formulation is done using the first order implicit method. An absolute convergence criterion of 10^{-4} was used for continuity equation while it was set to 10^{-5} for momentum and 10^{-8} for energy equation. Courant-Friedrichs-Lewy (CFL) criterion was used for calculating maximum time step for the stability of the solution. Hence, Courant number, ($Co = \Delta t U / \Delta x$ where Δx is the minimum grid spacing, U is the average fluid velocity and Δt is the time step size) was kept less than 1(~ 0.88) for all calculations and time step size was calculated based upon this criteria.

2.4 Grid Independence and validation

A grid independence test was carried out for five different grids with water as the working fluid at *Wo* = 6.65 and *L/D* = *2*. Figure 3 (a) shows the temporal variation of velocity at *r** = 0.5 and *z** = 2. It was found that all values lie within 0.25% range of the values obtained using Grid 2 (grid shown in Figure 2 (b)). Hence, all the further simulations were carried out using Grid 2 i.e. 50×200 having element size of 0.02. The time step size was kept to be 0.00025s meeting the CFL criterion with this grid size. Uchida [18] provided the analytical solutions for fully developed single-phase pulsating flow in a pipe. To validate the numerical technique and method, computational domain was extended so as to neglect the effect of meniscus and to allow the flow to become fully developed. For this purpose, *L/D* was chosen to be 40. The flow parameters and boundary conditions were chosen so as to match with those used by Uchida [18]. Hence, *Wo* was taken as 10 and *Re* was kept at 140 to maintain the laminar flow conditions. Figure 3 (b) compares the solutions obtained using the present technique and those provided by Uchida [18]. The difference in the solutions obtained using the present simulations and those of Uchida [18] are within ±2% range. Hence, the numerical technique and methods used in this study are considered satisfactory and promising, with reasonably high level of confidence.

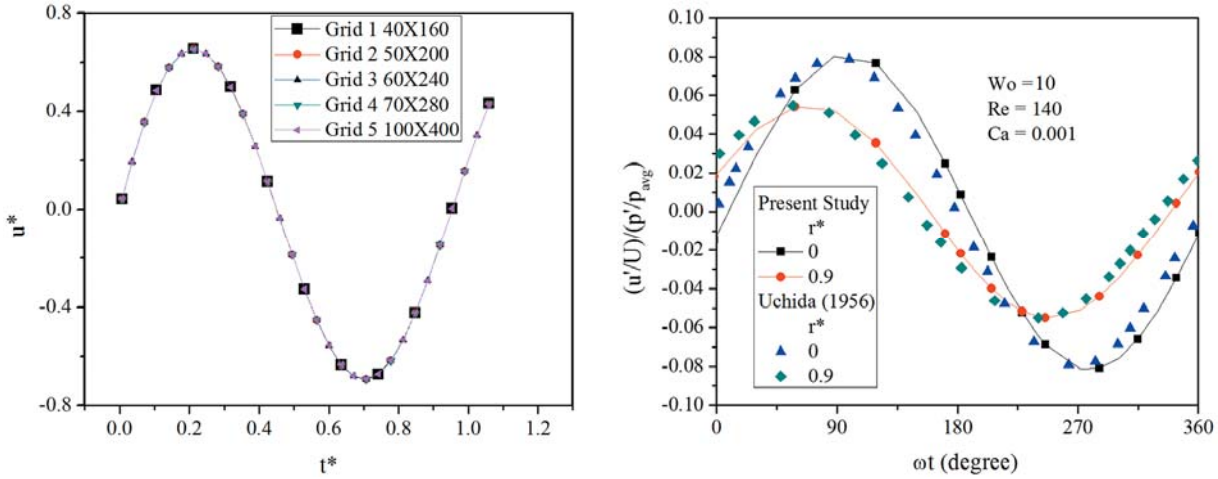

Figure 3: (a) Grid independence test for oscillating problem taking water as working fluid at *Wo* = 6.65, *L/D* = 2 with pure oscillations. (b) Validation of the present study with Uchida [18] solution of temporal variation of fluctuating component of velocity profile at different radial location.

3. RESULTS AND DISCUSSION

The results obtained from the simulations have been consolidated in this section. Firstly, we discuss the hydrodynamics of pulsating slug flow followed by a detailed analysis of the effect of pulsations on the heat transfer in pulsating slugs. The nuances of defining the time averaged Nusselt number have also been discussed.

3.1 Hydrodynamics of pulsating slug

Figure 4 shows the fluctuating velocity profile at different phase angles for various *Wo*. It is clear from the figure that at low frequency i.e. low *Wo*, velocity profiles slowly approach parabolic profile with maximum velocity at centre. Figure 4 (a) shows the fluctuating velocity profile for a time period at different radial location for *Wo* = 2.35. Imposition of low frequency does not have much effect on velocity profiles. As the frequency is increased, "annular effect" starts increasing at various phase angles. It means that the fluid near the wall oscillates as if it were a solid body, with the maximum amplitude of velocity. In Figure 4 (b), velocity is maximum near the wall rather than at centre for phase angle 7˚. This effect is pronounced at higher frequencies. At *Wo* = 6.65, annular effect can be seen at almost all phase angles. The velocity is maximum near the wall while smaller at centre. As classified by Ohmi et al. [19], the flow, in all these cases, lie in the intermediate regime of pulsating flows, which denotes the transition from steady to pulsatile field with observable influences of flow oscillation on flow field. With higher frequencies, the effect of pulsations becomes more and more confined in a narrow zone near the wall. This is why the fluctuating velocity is higher near the wall as compared to that in centre at higher frequencies. It evens starts to become negative with higher *Wo*. Another important thing to note down is the attenuation of the maximum fluctuating velocity with increasing frequency.

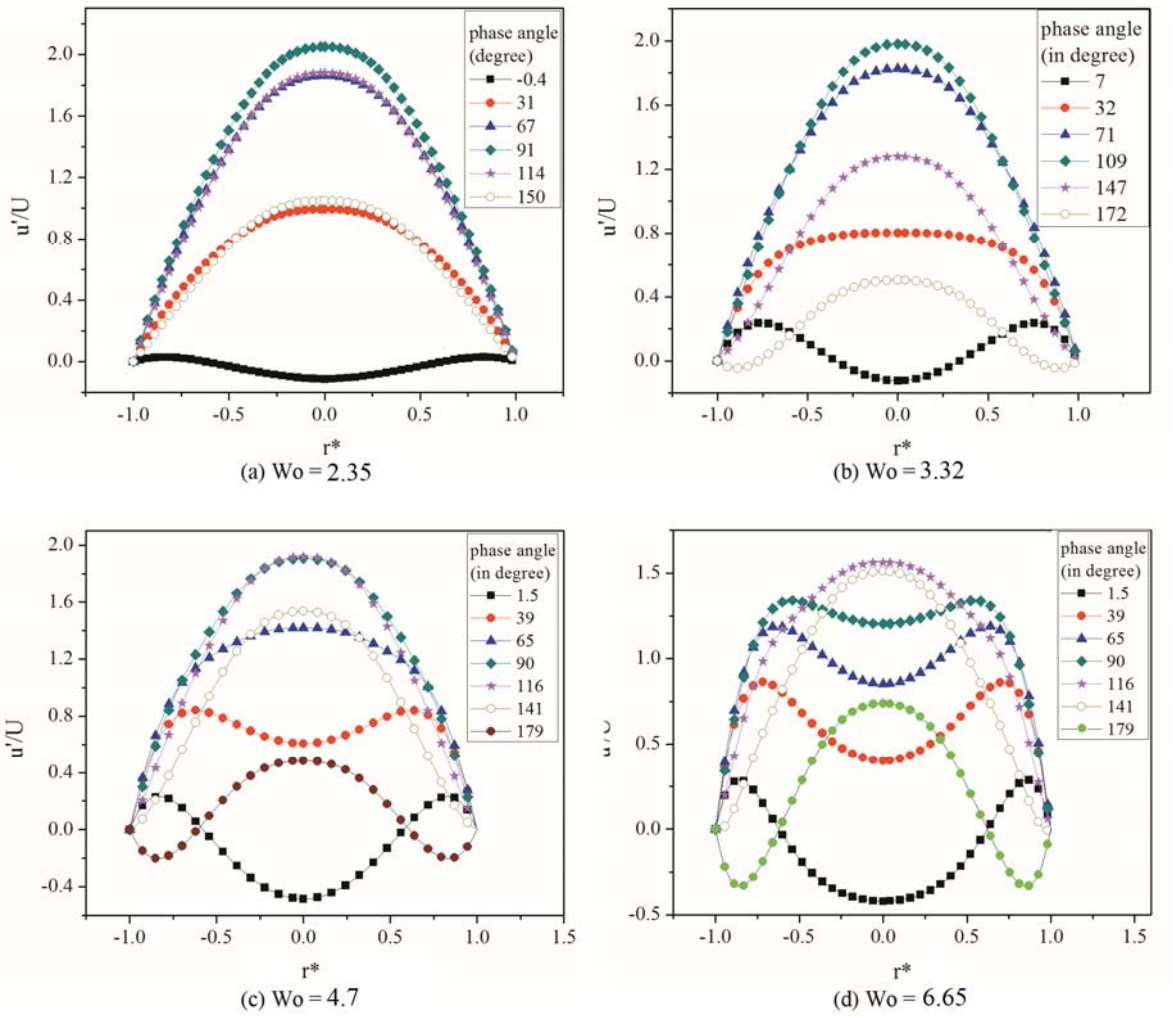

Figure 4: Fluctuating velocity profile at different phase angles for different *Wo*, (a) *Wo* = 2.35, (b) *Wo* = 3.32, (c) *Wo* = 4.7 and (d) *Wo* = 6.65.

Figure 5 shows the temporal variation of fluctuating velocity profile at different radial locations for one oscillating cycle at different *Wo*. At low *Wo*, velocities at different radial locations are in phase. As the frequency is increased, velocities at different radial locations also get shifted and hence a phase-lag between them is also observed while the fluctuating component keeps on decreasing with *Wo*. This phase shift between fluctuating velocities at different radial location is also a direct consequence of confined effect of oscillation near the wall. This is another reason because of which phase shift between radial locations near centre (r^* = 0 and0.2) is almost zero for all the frequencies. Because of the inertia of the fluid, a phase-lag between the pressure gradient and the fluctuating velocity exists which keeps on increasing with frequency and finally reaches an asymptotic value of 90˚ as clear from Figure 5. These observations are in conformity with the analytical results obtained by Uchida [18].

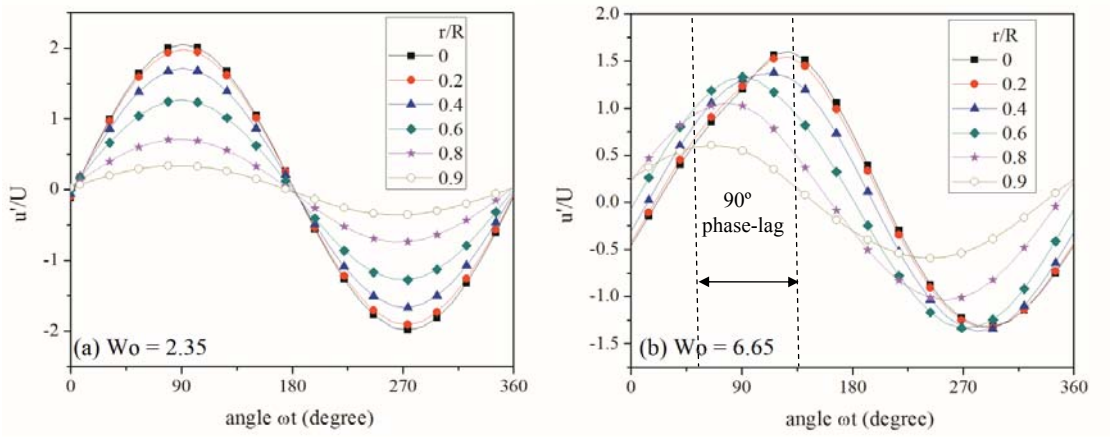

Figure 5: Temporal variation of fluctuating velocity profile at different radial locations for different *Wo* (a) *Wo* = 2.35 and (b) *Wo* = 6.65.

Figure 6 shows the contours of axial and radial components of velocity (relative) at various phases. The streamlines are also superimposed on the contours. The vortex migrates from one end of the slug to another in an oscillating fashion. It can be seen how the boundary layer starts developing at the beginning of each cycle. In a stationary frame of reference, it would be observed that the velocity is higher at the center of the tube away from the interface and gradually decreases towards the interface. The *u*-velocity is more near the axis away from the interface. The *v*-contours near the interface show higher magnitude due to circulation near the interface.

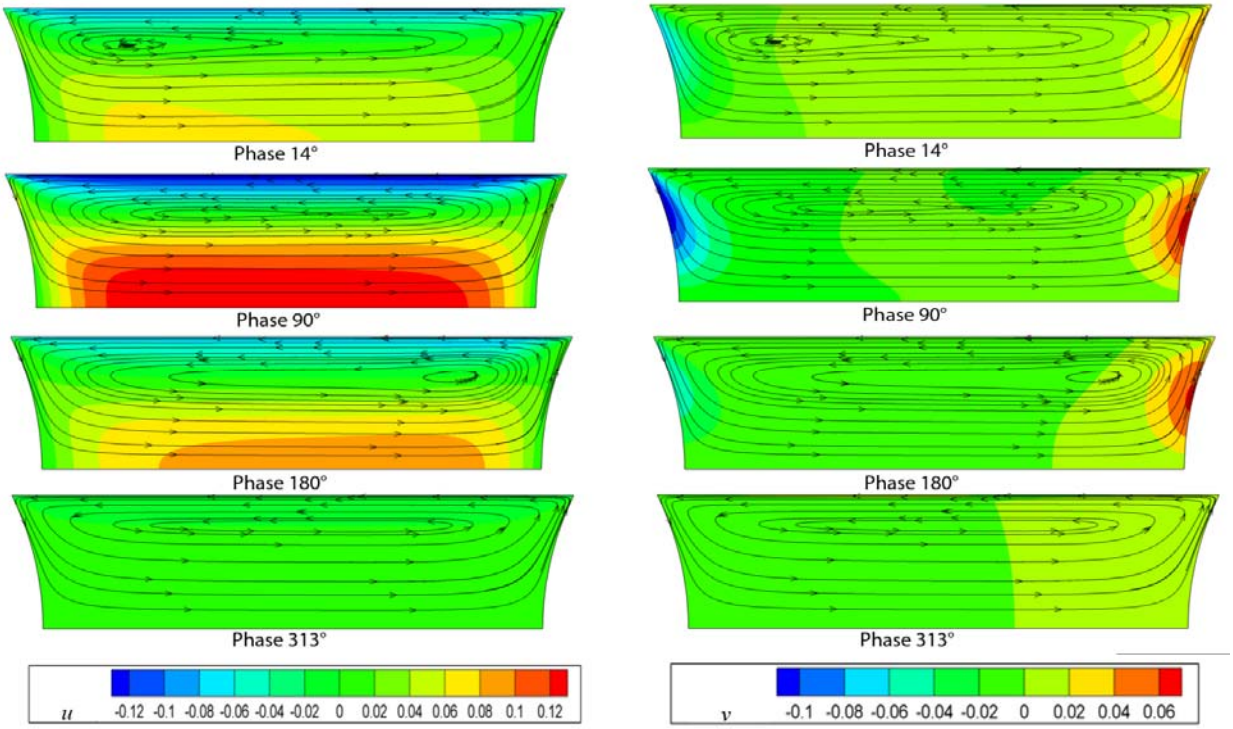

Figure 6: Contours of axial and radial components of velocity at various phase angles, along with the streamlines for *Wo*= 3.32, *L/D* = 2 and *Ca* = 0.001.

3.2 Heat Transfer

Figure 7 shows the streamlines and temperature contours for the water slug at various phase angles for a complete cycle for *Wo* = 3.32. Bajpai and Khandekar [9] found that there were strong internal circulations, which was the reason behind enhanced heat transfer for short slugs. Here, we try to understand the effect of pulsations on the heat transfer characteristics.

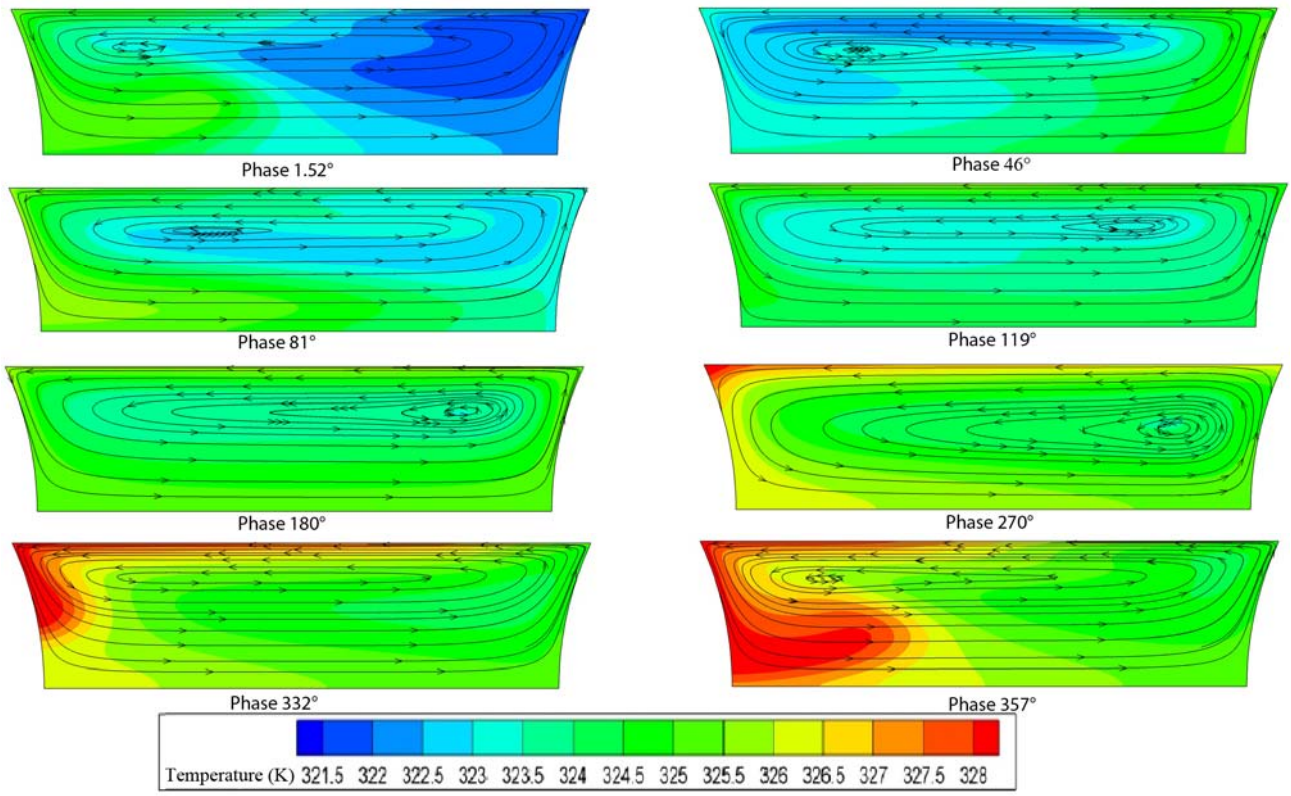

Figure 7: Temperature contours and streamlines at different phase angles for *Wo* = 3.32, *L/D* = 2 and *Ca* = 0.001.

It can be seen that a thermal boundary layer develops as the slug starts moving inside the capillary. As the cycle progresses, the hotter liquid near the wall is brought to the axis while the colder liquid goes towards the wall. Eventually, the colder liquid gets trapped within the core. One can see the variation of the local fluid temperature inside the slug at $z^* = 2$ at the start of the cycle in Figure 8 (a). As an interesting consequence of this, at the start of each cycle the energy gets distributed such that the temperature of the fluid towards the axis goes on increasing, which causes the overall bulk temperature of the fluid along certain vertical lines drawn normal to axis, to be greater than the local wall temperature. This gives rise to negative instantaneous *Nu* for certain locations along the axis during the beginning of the cycle where T_b becomes greater than T_w. In Figure 8 (b) it can be observed that, both, the average bulk fluid temperature and the wall temperature goes on increasing (as a consequence of constant heat flux boundary condition) but for a certain period of time at the beginning of each cycle, cross over each other. This apparent 'negative' *Nu* is an artifact of the definition of *Nu* used ($Nu = q''d/(k_f(T_w - T_b))$) since the temperature gradient at the wall is always positive (refer Figure 9), implying that heat always flows from the wall into the fluid. Hence, one needs to use the correct definition of *Nu* when dealing with pulsating flows. Negativity still exists for time-averaged local *Nu* but when the *Nu* is calculated by Eq. (13), time-averaged *Nu* becomes positive. Hemida et al. [20] constructed this definition of time averaged *Nu* which not only had a physical significance but also was beneficial from an engineering point of view.

The instantaneous Nusselt number and its average were defined earlier by Kim et al. [21] as:

$$Nu = D\partial\left[(T - T_{inlet})/(T_w - T_{inlet})\right]/\partial y'\big|_{y'=D} \tag{10}$$

$$Nu_o = 1/\theta \int_0^\theta Nu\,dt \tag{11}$$

Hemida et al. [20] argued that if both numerator and denominator were time varying, a more elaborate analysis of the time averaged Nusselt number is required. They defined the time average *Nu* based on the time average heat transfer coefficient h_o and asserted that the definition should satisfy the Newton's law of cooling ($q'' = h_o(T_{wo} - T_{bo})$, where T_{wo} and T_{bo} are time averaged wall and bulk temperatures respectively) and hence, yield a heat flux value compatible with the energy equation. They went on to integrate the energy equation and after a series of simplifications (Refer Hemida et al. [21]), obtained the final general expression of h_o as:

$$h_o = \frac{k_f}{\theta} \frac{\int_0^\theta n \cdot \nabla T\big|_w \, d\theta}{(T_{wo} - T_{bo})} \tag{12}$$

Simplifying the above expression for a constant heat flux boundary condition, the time averaged *Nu* was given as:

$$Nu_{ta} = \frac{q''d}{k_f} \cdot \frac{1}{(T_{wo} - T_{bo})} \tag{13}$$

where, T_{wo} and T_{bo} are defined as:

$$T_{wo} = \frac{1}{\theta}\int_0^\theta T_w(t)dt \qquad \text{and} \qquad T_{bo} = \frac{\int_0^\theta \int_A |u| T \cdot dA dt}{\int_0^\theta \int_A |u| \cdot dA dt} \tag{14}$$

$$Nu_m = \int_0^L Nu_{ta}(z)dz \tag{15}$$

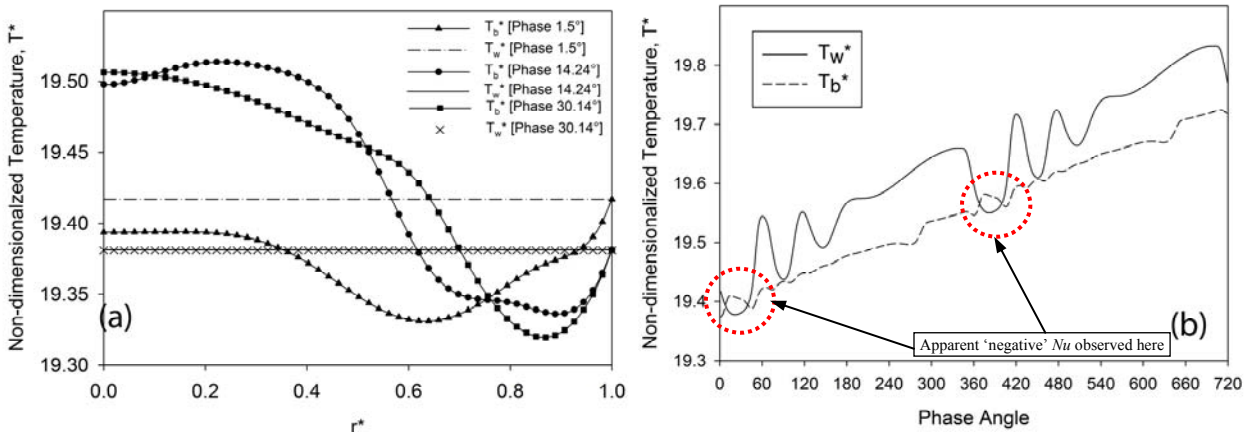

Figure 8: (a) Variation of temperature along radial direction for certain phase angles for $z^* = 2$. (b) Temporal variation of wall and bulk temperature for $z^* = 2$ for $Wo = 3.32$.

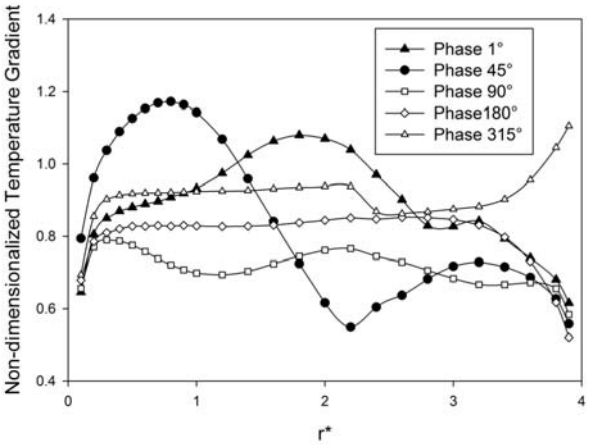

Figure 9: Axial variation of temperature gradient at the wall during a cycle at $Wo = 6.65$.

Using the above expression, we find the time averaged Nusselt number $Nu_{ta,}$ for different Womersley numbers. It is observed that there is not much enhancement in $Nu_{m,}$ rather there is a conditional reduction in

Nu_m as a result of the imposed flow pulsations. At higher frequency, one can observe a certain degree of enhancement Nu_m. Figure 10 (a) shows that the enhancement is mainly in the thermally developing zone of the slug, i.e., from where the thermal boundary layer grows.

Imposing pulsations disturbs the flow which alters the thermal and hydrodynamic boundary layer. Subsequently, it affects the inter-particle momentum and energy exchange. Due to this enhanced mixing, augmentation in heat transfer is expected. Many researchers in the past have investigated the effect of imposing pulsations, of sinusoidal or square waveform, over steady, single-phase laminar flows for constant temperature or constant heat flux boundary conditions (for example, see Hemida et al. [20], Brereton et al. [22], Mehta & Khandekar [23, 24]). Having studied the effect of various parameters like *Re*, frequency of pulsations, amplitude of pulsations and Prandtl number, they concurred that pulsations do not have any significant effect on the heat transfer characteristics for the case of single-phase pulsating flows.

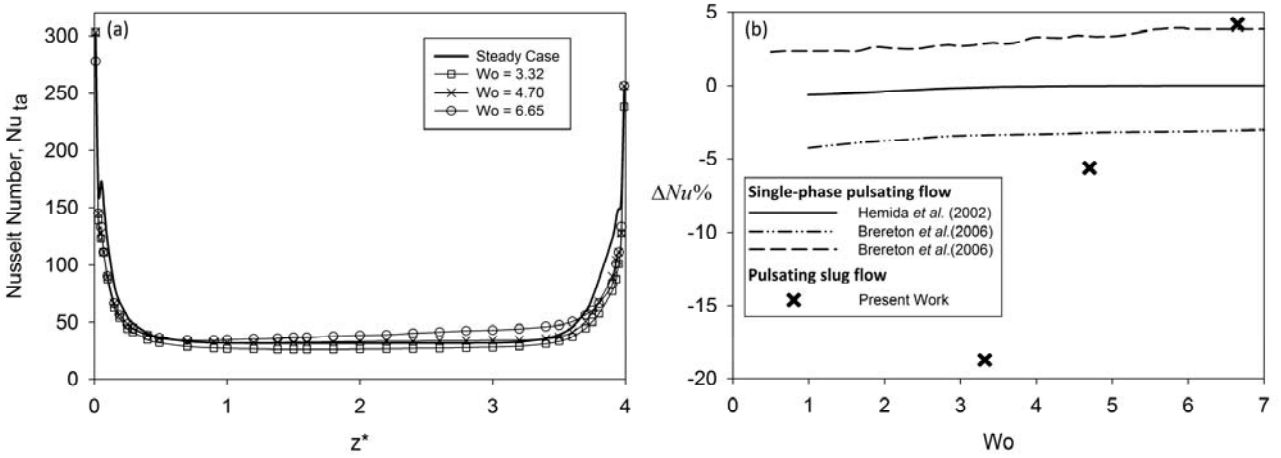

Figure 10: (a) Axial variation of time averaged Nusselt Number for different *Wo*. (b) Nusselt Number enhancement from its steady state value for different *Wo*. Here, results for the case of pulsating slug flow are compared with the results for pulsating single-phase available in literature.

Present results are quite similar to the ones found in literature for pulsating single-phase flows. Figure 10 (b) shows the results of various researchers for single-phase pulsating flow, compared with the results for the present case of pulsating slug flow. Qualitatively one could observe that the nature of variation is similar for both pulsating single-phase and pulsating slug flow, i.e. a negligible enhancement rather deterioration in heat transfer is exhibited. It shows that the percentage change in Nusselt number depends upon the frequency. In the present case, for *Wo* = 3.32 and 4.7, mean *Nu* is lower than the steady slug flow, while for *Wo* = 6.65, the mean *Nu* has marginally improved.

5. SUMMARY AND CONCLUSIONS

Fluid flow and heat transfer in an isolated dry slug pulsating uni-directionally inside a capillary tube has been investigated numerically. The frequency range chosen is typically found in a PHP. The simplified analysis presented in this work gives some insight into the otherwise complex PHPs. It is observed that low frequency does not have much effect on the velocity profile. A nearly parabolic profile of fluctuating velocity is observed in this case. As the pulsation frequency is increased, the flow starts shifting from parabolic to annular. In this case, the maximum velocity is found near the wall and not at the axis of the plug. As frequency is increased, a phase shift between oscillating velocities at different radial locations is observed. The effect of pulsations on time averaged *Nu* is insignificant. At the higher end of the frequency range, small enhancement (< 5%) is observed. Hence, it can be concluded that if the existence of thin liquid film and resulting slip are excluded in the analysis of PHP, then just because of liquid slug pulsations, enhancement in heat transfer is practically absent.

NOMENCLATURE

A cross-sectional area, m^2
c_p specific heat at constant pressure, J/kg-K
D,d diameter, m
D_h hydraulic diameter, m
h heat transfer co-efficient, $W/m^2 K$

g acceleration due to gravity, m/s^2
k thermal conductivity, W/m K
L characteristic length, m
q" heat flux, W/m^2
r coordinates normal to the flow
R radius, m
T temperature, K
t time, s
U velocity, m/s
z coordinates along the flow

Greek symbols

α thermal diffusivity, m^2/s
μ dynamic viscosity, Pa-s
ν kinematic viscosity, m^2/s
ρ density, kg/m^3
θ time period, s
ω frequency
σ surface tension, N/m

Dimensionless numbers

Bo Bond number ($\Delta\rho \cdot g \cdot L^2/\sigma$)
Ca Capillary number ($\mu \cdot U/\sigma$)
Nu Nusselt number ($h \cdot D/k_f$)
Pr Prandlt number (ν/α)
Re Reynolds number ($\rho \cdot U \cdot D/\mu$)
Wo Womersley number ($R \cdot (\omega/\nu)^{0.5}$)

Subscripts

b bulk
f fluid
h hydraulic
m mean
o,ta time averaged quantity
w wall

ACKNOWLEDGEMENTS

Financial grants from the Indo-French Center for Promotion of Advanced Research (IFCAR) are gratefully acknowledged.

REFERENCES AND CITATIONS

[1] Khandekar, S. & Groll, M. (2004). An insight into thermo-hydraulic coupling in pulsating heat pipes, *International Journal of Thermal Sciences,* **43(1)**, 13-20.

[2] Khandekar, S. (2004). Thermo-hydrodynamics of closed loop pulsating heat pipes.(Doctoral dissertation). Institute of Nuclear Engineering & Energy Systems (IKE), University of Stuttgart, Germany. (Available at: http://elib.uni-stuttgart.de/opus/volltexte/2004/1939/)

[3] Rao, M., Lefevre, F., Khandekar, S. & Bonjour, J. (2013). Understanding transport mechanism of a self-sustained thermally driven oscillating two-phase system in a capillary tube. *International Journal of Heat and Mass Transfer*, **65**, 451-459.

[4] Khandekar, S., Gautam, A.P. & Sharma, P.K. (2009). Multiple quasi-steady states in a closed loop pulsating heat pipe. *International Journal of Thermal Sciences,* **48**, 535-546.

[5] Zhang, H. & Faghiri, A. (2008). Advances and unsolved issues in pulsating heat pipes. *International Journal of Heat and Mass Transfer,* **23(1)***,* 20-44.

[6] Walsh, P.A., Walsh, E.J. & Muzychka, Y.S. (2010). Heat transfer model for gas–liquid slug flows under constant flux. *International Journal of Heat and Mass Transfer,* **53**, 3193-3201.

[7] Gupta, R., Fletcher, D.F. & Haynes, B.S.(2010). CFD modelling of flow and heat transfer in the Taylor flow regime. *Chemical Engineering Science,* **65**, 2094-2107.

[8] Asadolahi, A.N., Gupta, R., Fletcher, D.F. & Haynes, B.S. (2011). CFD approaches for the simulation of hydrodynamics and heat transfer in Taylor flow. *Chemical Engineering Science,* **66**, 5575-5584.

[9] Bajpai, A.K. & Khandekar S.(2012). Thermal transport behavior of a liquid plug moving inside a dry capillary tube. *Heat Pipe Science and Technology,* **3**, 97-124.

[10] Mehdizadeh, A., Sherif, S.A. & Lear, W.E. (2011). Numerical simulation of thermofluid characteristics of two-phase slug flow in microchannels. *International Journal of Heat and Mass Transfer,* **54**, 3457-3465.

[11] Asadolahi, A.N., Gupta, R., Leung, S.S.Y., Fletcher, D.F. & Haynes, B.S. (2012). Validation of a CFD model of Taylor flow hydrodynamics and heat transfer. *Chemical Engineering Science,* **69**, 541-552.

[12] Talimi, V., Muzychka, Y.S. & Kocabiyik, S. (2012). Numerical simulation of the pressure drop and heat transfer of two-phase slug flows in microtubes using moving frame of reference technique. *International Journal of Heat and Mass Transfer*, **55**, 6463-6472.

[13] Talimi, V., Muzychka, Y.S. & Kocabiyik, S. (2013). Slug flow heat transfer in square microchannels. *International Journal of Heat and Mass Transfer*, **62**, 752-760.

[14] Leung, S.S.Y., Gupta, R., Fletcher, D.F. & Haynes, B.S.(2012). Gravitational effect on Taylor flow in horizontal microchannels. *Chemical Engineering Science,* **69**, 553-564.

[15] Zaloha, P., Kristal, J., Jiricny, V., Völkel, N., Xuereb, C. & Aubin, J.(2012). Characteristics of liquid slugs in gas–liquid Taylor flow in microchannels. *Chemical Engineering Science,* **68**, 640-649.

[16] Das, S.P., Nikolayev, V.S., Lefevre, F., Pottier, B., Khandekar, S. & Bonjour, J. (2010). Thermally induced two-phase oscillating flow inside a capillary tube. *International Journal of Heat and Mass Transfer,* **53**, 3905-3913.

[17] Mehta, B. & Khandekar, S. (2014). Taylor bubble-train flows and heat transfer in the context of Pulsating Heat Pipes. *International Journal of Heat and Mass Transfer,* **79**, 279-290.

[18] Uchida, S. (1956) The pulsating viscous flow superposed on the steady laminar motion of incompressible fluid in a circular pipe. *Journal of Applied Mathematics and Physics,***7**, 403-422.

[19] Ohmi, M., Iguchi, M. & Usui, T. (1981). Flow pattern and frictional losses in pulsating pipe flow. Part5: Wall shear stress and flow pattern in a laminar flow, *Bulletin of JSME*, **24** (187).

[20] Hemida, H.N., Sabry, M.N., Abdel-Rahim, A. & Mansour, H. (2002). Theoretical analysis of heat transfer in laminar pulsating flow. *International Journal Heat and Mass Transfer,* **45**, 1767-1780.

[21] Kim, S.Y., Kang, B.H., Hyun, J.M. (1993). Heat transfer in the thermally developing region of a pulsating channel flow. *International Journal of Heat and Mass Transfer,* **36**, 4257-4266.

[22] Brereton, G.J. & Jiang, Y.(2006). Convective heat transfer in unsteady laminar parallel flows. *Physics of Fluids,* **103602**, 1-15.

[23] Mehta, B. & Khandekar, S. (2010). Effect of periodic pulsations on heat transfer in simultaneously developing laminar flows: A numerical study. *Proc. 14th International Heat Transfer Conference,* August 8-13, 2010, Washington DC (USA).

[24] Mehta, B. & Khandekar, S. (2013). Local experimental heat transfer of single-phase pulsating flow in square mini-channel. *Proc. 4th International Micro/Nanoscale Heat and Mass Transfer Conference,* December 11-14, 2013, Hong Kong (China).

